

Multimodal Imaging of Spike Propagation: A Technical Case Report

CASE REPORT

N. Tanaka
P.E. Grant
N. Suzuki
J.R. Madsen
A.M. Bergin
M.S. Hämläinen
S.M. Stuffelbeam



SUMMARY: We report an 11-year-old boy with intractable epilepsy, who had cortical dysplasia in the right superior frontal gyrus. Spatiotemporal source analysis of MEG and EEG spikes demonstrated a similar time course of spike propagation from the superior to inferior frontal gyri, as observed on intracranial EEG. The tractography reconstructed from DTI showed a fiber connection between these areas. Our multimodal approach demonstrates spike propagation and a white matter tract guiding the propagation.

ABBREVIATIONS: EEG = electroencephalography; FLASH = fast low-angle shot; IEEG = intracranial electroencephalography; MEG = magnetoencephalography; MPRAGE = magnetization-prepared rapid acquisition of gradient echo

Detecting propagation of epileptic activity is critical for the care of neurosurgical patients with epilepsy. IEEG has been considered a criterion standard for investigating it,¹ whereas several researchers have reported that spatiotemporal source analysis of MEG and scalp EEG also can be useful.^{2,3} However, these studies did not incorporate anatomic pathways of propagation.

This case report describes the usefulness of a multimodal neuroimaging approach for representing spike propagation. We analyzed MEG/EEG spikes with a spatiotemporally distributed source model in a patient with frontal lobe epilepsy and compared the time course of the spikes with that of IEEG spikes. We also performed tractographic analysis of DTI data, to determine if the rapid propagation could be explained by a well-defined fiber connection between the onset and propagated areas of the spikes. We analyzed the data retrospectively.

Case Report/Technique

The patient was an 11-year-old boy with medically intractable epilepsy. Seizure onset was at age 4. His seizure semiology suggested that the right sensorimotor cortex for the left upper extremity was involved during ictal activity. Interictal EEG showed midline frontocentral spikes that were dominant on the right electrodes. A right superior frontal gyrus cortical dysplasia was identified on MR imaging (Fig 1A).

MEG was recorded with a 306-channel whole-head MEG system (Vectorview, Elekta Neuromag, Helsinki, Finland). EEG was simultaneously recorded with a 70-channel electrode cap, based on the 10–10 electrode-placement system. The sampling rate was 600 Hz,

and the data were digitally filtered at 1–40 Hz for analysis. High-resolution 3T MR imaging data were acquired by using a 32-channel head coil with MPRAGE (TE = 3.37 ms, TR = 2000 ms, flip angle = 9°, voxel size = 1 × 1 × 1 mm) and multiecho FLASH pulse sequences (TE = 1.89 ms, TR = 20 ms, flip angle = 5°, voxel size = 1 × 1 × 1 mm) (Magnetom Trio; Siemens, Erlangen, Germany). We also acquired DTI sequences (60 gradient directions, TE = 82 ms, TR = 7850 ms, flip angle = 90°, section thickness = 2 mm, voxel size = 2 × 2 × 2 mm, diffusion sensitivity of $b = 700$ s/mm). IEEG was recorded by using grids and strips in the right medial and lateral frontal surfaces, covering the right superior and inferior frontal gyri (Fig 1C; XLTEK EEG system; Excel-Tech, Oakville, Canada). No depth electrodes were used. The sampling rate was 512 Hz, and the data were low-pass filtered at 30 Hz for analysis. The patient underwent CT after implantation of intracranial electrodes to confirm their location (voxel size = 0.5 × 0.5 × 0.5 mm).

We analyzed 50 spikes appearing simultaneously on MEG and EEG. Spatiotemporal source distribution was calculated by using a minimum norm estimate.⁴ We obtained a 3-layer head model from MPRAGE and FLASH MR imaging sequences by a boundary elemental method.⁵ The inverse solution was calculated from the forward solution, which models the signal-intensity pattern generated by a unit dipole distributed on the MR imaging–derived cortical surface.^{6,7} The activation at each location was mapped at each time point of the spikes by using this inverse solution. For IEEG, we determined 2 active frequently spiking intracranial electrodes in each area of the superior and inferior frontal gyri. The largest time difference between the superior and inferior peaks at these electrodes was obtained from 50 spikes.

We coregistered the CT images onto the cortical surface and determined the location of the sites corresponding to the active intracranial electrodes (Fig 1C). Source waveforms of each MEG spike were extracted from the spatiotemporal source distribution at the sites of inferior frontal gyrus active electrodes. EEG source waveforms at the sites of the superior frontal gyrus electrodes were extracted in the same manner. We obtained the time differences of the peaks of MEG and EEG source waveforms for each spike.

For fiber tracking, we performed a tractographic analysis of DTI data by using TrackVis software (Wang and Wedeen, www.trackvis.org). This algorithm uses the standard fiber assignment by the continuous tracking method⁸ and calculates all possible fiber connections in the whole brain. Next we put an anatomic region of interest in the

Received March 26, 2011; accepted after revision April 24.

From the Athinoula A. Martinos Center for Biomedical Imaging, (N.T., N.S., M.S.H., S.M.S.), Massachusetts General Hospital, Charlestown, Massachusetts; and Departments of Radiology (P.E.G.), Neurosurgery (J.R.M.), and Neurology (A.M.B.), Children's Hospital Boston, Boston, Massachusetts.

This work was supported by the National Institutes of Health (P41RR14075, R01NS037462-07), Mental Illness and Neuroscience Discovery Institute, National Alliance for Research on Schizophrenia and Depression Young Investigators Award, and Japan Epilepsy Research Foundation.

Please address correspondence to Naoaki Tanaka, MD, Athinoula A. Martinos Center for Biomedical Imaging, 149 Thirteenth St, Suite 2301, Charlestown, Massachusetts 02129; e-mail: naoro@nmr.mgh.harvard.edu



Indicates open access to non-subscribers at www.ajnr.org

<http://dx.doi.org/10.3174/ajnr.A2701>

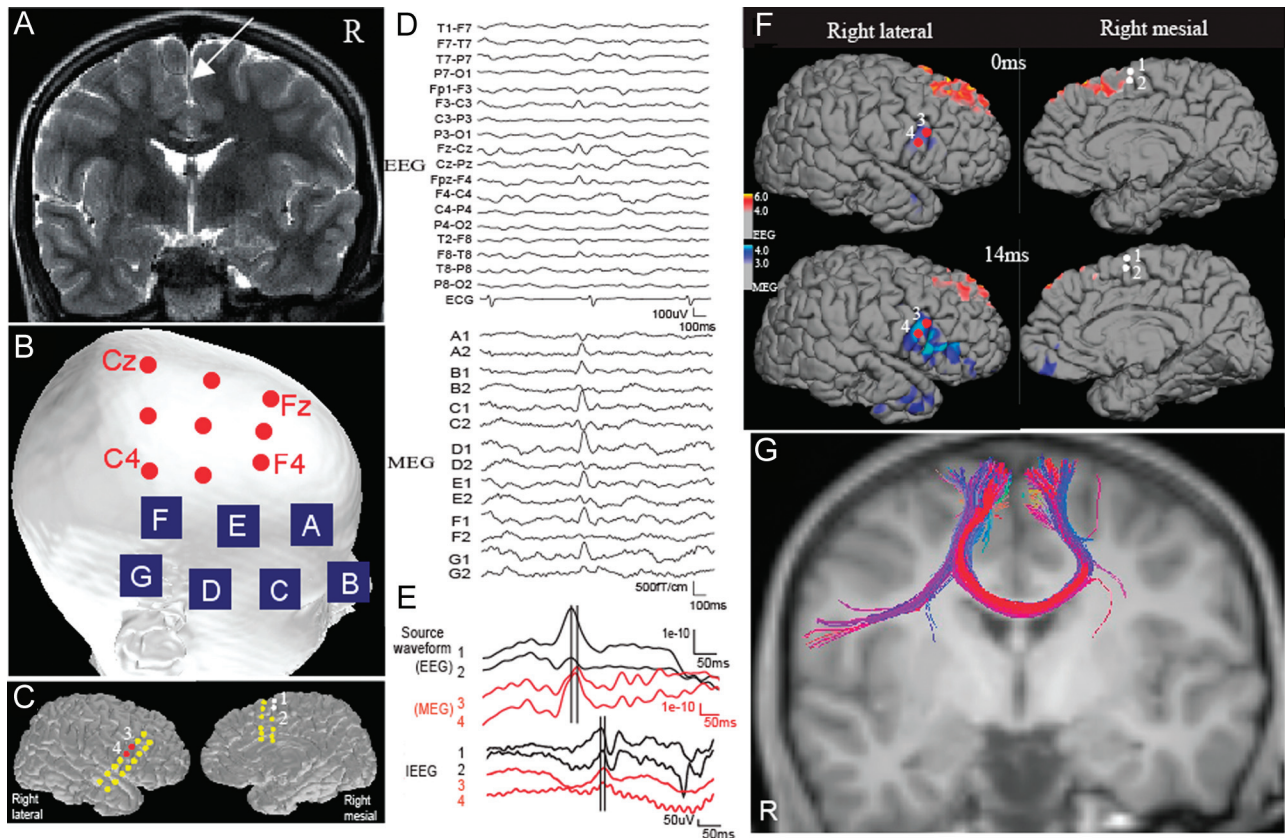


Fig 1. *A*, MR image shows a right superior frontal gyrus lesion (arrow). *B*, Active sites that show frequent spikes on EEG and MEG. Red circles and blue squares show EEG electrodes and MEG sensors, respectively. Note that the active MEG electrodes are located more inferiorly than the active EEG electrodes. *C*, The location of grids is shown on the cortical surface. *D*, A typical spike recorded on simultaneous EEG and MEG. The labels of the MEG channels correspond to the sensors shown on *B*. Each site has 2 gradiometers. *E*, Source waveforms of an EEG/MEG spike and a typical spike on IIEEG. Source waveforms are extracted at sites 1 and 2 (superior frontal) for EEG and 3 and 4 (inferior frontal) for MEG. The superior frontal peak of EEG waveforms precedes the inferior frontal peak of MEG waveforms by approximately 20 ms. A similar time difference is seen on the IIEEG spike. *F*, A source distribution map of a typical spike appearing on both EEG and MEG. Cortical activation is shown with red/yellow for EEG and blue/dark blue for MEG. The EEG activation appears in the right superior frontal area at the early latency (0 ms), whereas the MEG source shows later activation in the inferior frontal area (14 ms). White and red circles show the location of active IIEEG electrodes in the superior (sites 1 and 2) and inferior (sites 3 and 4) frontal areas, respectively. *G*, The tractography shows a fiber connection between the right superior and inferior frontal gyri.

dorsal part of the lesion and the contralateral region (Fig 1G). The tractographic map was coregistered onto the MPRAGE images.

Results

EEG spikes were identified in the superior frontal electrodes, maximally at F4 and Fz, whereas MEG spikes were mainly seen in the inferior frontal sensors (Fig 1B, -D). Spatiotemporal source maps of EEG and MEG spikes showed right superior and inferior frontal activation, respectively (Fig 1F). The peaks of EEG source waveforms at the superior frontal sites preceded those of MEG source waveforms at the inferior frontal sites by 8–96 ms (mean, 29 ms) (Fig 1E). Similarly, superior frontal peaks of IIEEG spikes preceded inferior frontal peaks by 3–98 ms (mean, 36 ms) (Fig 1D). The time differences on IIEEG and MEG/EEG were similar without any statistical difference ($P > .05$, paired t test). The tractography showed a well-defined fiber connection between the right superior and inferior frontal areas (Fig 1G). This connection was not observed on the contralateral side (Fig 1G).

The patient underwent a lesionectomy, with a partial resection of the frontal lobe, and has been seizure-free for 10 months after surgery.

Discussion

In the present case, IIEEG spikes showed superior frontal peaks followed by inferior frontal peaks, suggesting spike propagation from the superior-to-inferior frontal gyri. The time difference of the peaks between these areas was similar on MEG/EEG source waveforms and IIEEG. These results suggest that spatiotemporal source analysis can represent spike propagation as observed on IIEEG.

Several researchers have reported that spatiotemporal source analysis of MEG represents spike propagation in the inferior frontal cortex on MEG.³ On the other hand, MEG is less sensitive than EEG in the medial surface of the superior frontal gyrus.⁹ In the present case, EEG and MEG represented well early activation in the superior frontal gyrus and propagation in the inferior frontal gyrus, respectively. These results nicely demonstrate the complementary role of MEG and EEG for investigating the spike propagation.

Generally, spatiotemporal source analysis calculates the source distribution that can reconstruct the original signals on the sensors at each time point. It does not incorporate any information of anatomic pathways. In this case, the tractography showed a fiber connection between the superior/inferior frontal gyri by putting a region of interest in

the structural lesion, connecting the areas that showed activation associated with spike propagation in minimum norm estimate maps. Fiber tractography may reflect the structural pathway associated with spike propagation.

In conclusion, spatiotemporal source analysis of MEG/EEG spikes and tractographic analysis of DTI aid in identifying the epileptic discharge site and show spike propagation via a specific white matter tract. The multimodal approach provides functional and structural information associated with the pathophysiologic neural network in epilepsy.

References

1. Alarcon G, Garcia Seoane JJ, Binnie CD, et al. **Origin and propagation of interictal discharges in the acute electrocorticogram: implications for pathophysiology and surgical treatment of temporal lobe epilepsy.** *Brain* 1997;120:2259–82
2. Zumsteg D, Friedman A, Wieser HG, et al. **Propagation of interictal discharges in temporal lobe epilepsy: correlation of spatiotemporal mapping with intracranial foramen ovale electrode recordings.** *Clin Neurophysiol* 2006;117:2615–26
3. Tanaka N, Hämäläinen MS, Ahlfors SP, et al. **Propagation of epileptic spikes reconstructed from spatiotemporal magnetoencephalographic and electroencephalographic source analysis.** *Neuroimage* 2010;50:217–22
4. Hämäläinen MS, Ilmoniemi RJ. **Interpreting magnetic fields of the brain: minimum norm estimates.** *Med Biol Eng Comput* 1994;32:35–42
5. Hämäläinen M, Sarvas J. **Realistic conductivity geometry model of the human head for interpretation of neuromagnetic data.** *IEEE Trans Biomed Eng* 1989;36:165–71
6. Dale AM, Fischl B, Sereno MI. **Cortical surface-based analysis. I. Segmentation and surface reconstruction.** *Neuroimage* 1999;9:179–94
7. Fischl B, Sereno MI, Dale AM. **Cortical surface-based analysis. II. Inflation, flattening, a surface-based coordinate system.** *Neuroimage* 1999;9:195–207
8. Mori S, Crain BJ, Chacko VP, et al. **Three-dimensional tracking of axonal projections in the brain by magnetic resonance imaging.** *Ann Neurol* 1999;45:265–69
9. Goldenholz DM, Ahlfors SP, Hämäläinen MS, et al. **Mapping the signal-to-noise-ratios of cortical sources in magnetoencephalography and electroencephalography.** *Hum Brain Map* 2009;30:1077–86